Laser-Ultrasound with periodic excitation pattern for simultaneous measurement of thickness, longitudinal- and transverse sound speeds in plates

Georg Watzl[1], Clemens Grünsteidl[1]
[1] *Research Center for Non Destructive Testing GmbH, 4040 Linz, Österreich*

Introduction

Ultrasonic techniques to measure the thickness of a sample typically require its sound speed as a priori knowledge, or vice versa. However, there are situations in which the sound speed is not precisely known, e.g. when it is influenced by temperature and thus a precise thickness measurement is not possible. To overcome this limitation, we use laser-ultrasound to simultaneously generate and detect plate resonances and a surface acoustic wave with a specific wavenumber. As a contact-free method, laser-ultrasound can be applied in challenging measurement environments, such as on hot or moving objects, requires no coupling fluid and is well suited for automation [1, 2]. Additionally the excitation and detection geometry can be easily manipulated by optical means. In our case the excitation laser is focused to a periodic line pattern, where the line spacing dictates the wavenumber of the generated surface acoustic wave. The overall size of the pattern is chosen small enough such that additional simultaneous coupling into plate resonances is achieved in a single measurement. From the frequencies of two plate resonances and the frequency of the surface acoustic wave at the wavenumber given by the pattern, thickness and both sound speeds of the plate can be calculated. We provide experimental demonstrations for the complete elastic characterization and thickness measurement of isotropic plates with non-constant thickness or varying elastic properties due to heating.

Theory

The possible vibration states of an isotropic plate are determined by the Rayleigh-Lamb equations [3]:

$$\frac{\tan(\beta h/2)}{\tan(\alpha h/2)} + \left(\frac{4k^2\alpha\beta}{(\beta^2-k^2)^2}\right)^{\pm 1} = 0\,, \qquad (1)$$

where $\alpha = \sqrt{(\omega/c_\mathrm{L})^2 - k^2}$, $\beta = \sqrt{(\omega/c_\mathrm{T})^2 - k^2}$, $\omega = 2\pi f$, and h is the thickness of the plate. Thus, the vibration characteristics of an isotropic plate are fully determined by its thickness and the elastic properties given by the longitudinal sound speed c_L and transverse sound speed c_T.

All combinations of vibration frequency f and wavenumber k, which satisfy equation 1 form the free vibrational modes of the plate. These can be determined by numerical methods and are represented in dispersion diagrams (see Figure 1). Our method is based on discrete points in those curves:

Zero-group-velocity modes

Vibrational modes without group velocity do not transport energy along the plate surface and therefore form long-ringing resonances near the excitation region. This corresponds to points in the dispersion curves (Figure 1), where the mode's slope $(\partial f/\partial k)_\mathrm{res} = 0$.

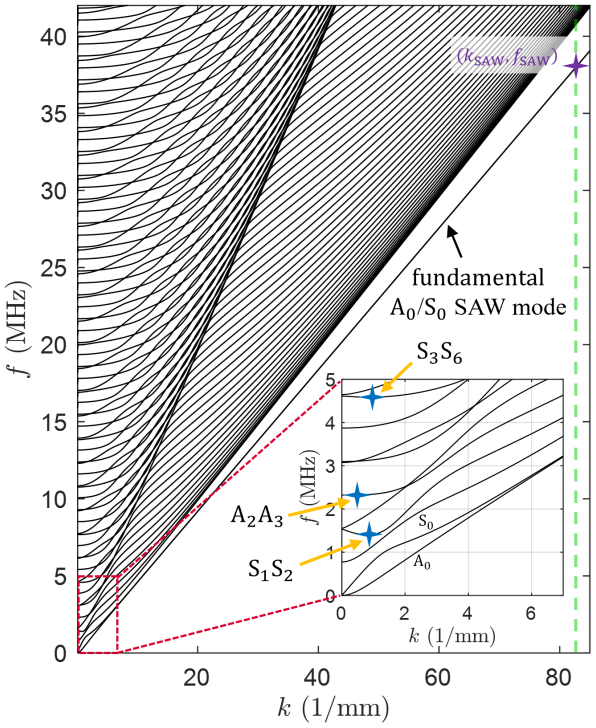

Figure 1: Dispersion curves of a 2 mm thick isotropic aluminum plate with a Poisson's ratio of $\nu = 0.33$.

Resonances with $k \neq 0$, which are called zero-group-velocity (ZGV) resonances [4], are locally confined standing waves. The locations of the S_1S_2, A_2A_3, and S_3S_6 ZGV resonances of an aluminum plate are displayed in the enlarged section in Fig. 1. The designation of the ZGV modes is based on reference [4].

It has been shown, that ZGV resonances can be measured exceptionally well with LUS [5, 6]. Moreover, by measuring at least two ZGV resonance frequencies, the Poisson's ratio of the plate can be determined without the need to know the thickness [7, 2, 8]. This concept is used in our method and combined with information gained from an additional point in the dispersion curves:

Fundamental A_0/S_0 mode, SAW mode

At wavelengths ($\lambda = 2\pi/k$) $\ll h$, the symmetric and antisymmetric zero-order modes (S_0, A_0) converge. In this higher frequency region, these oscillations are approximately equivalent to a Rayleigh- or surface acoustic wave

(SAW), which propagates only near the surface with an almost constant phase velocity of $c_{\mathrm{SAW}} = 2\pi f_{\mathrm{SAW}}/k_{\mathrm{SAW}}$, where k_{SAW} and f_{SAW} are a specific point on the dispersion curve of the fundamental A_0/S_0 mode (see Figure 1). Using a periodic line excitation pattern with line spacing λ_{pat}, SAWs of specific wavenumber $k_{\mathrm{SAW}} = 2\pi/\lambda_{\mathrm{pat}}$ matching the periodicity can be excited [9, 10], and its corresponding frequency f_{SAW} can be measured. Although higher order modes with wavenumber k_{SAW} are also excited (green dashed line in Figure 1), they typically have lower amplitude and are easily separable due to their different propagation speeds and the frequency gap to the SAW. Various approximation formulas exist by which the SAW speed c_{SAW} can be determined via the Poisson's ratio ν and the transverse sound speed c_{T} [11].

If the total size of the pattern used for SAW excitation d is considerably smaller than the ZGV wavelengths, the ZGV waves emitted from each individual line of the pattern still interfere largely constructively with each other. This enables simultaneous excitation of a specific SAW (purple cross in Figure 1) and ZGV resonances. Given adequate signal-to-noise ratio, at least two ZGV resonances f_{ZGV1}, f_{ZGV2} and f_{SAW} can be gained from one single laser pulse.

Determination of c_{L}, c_{T} and h

From the 3 measured frequencies f_{ZGV1}, f_{ZGV1}, and f_{SAW}, and with additional knowledge on the SAW wavenumber k_{SAW}, the plate's properties c_{L}, c_{T}, and h are found as follows:

The Poisson's number ν can be calculated from the ratio between f_{ZGV1} and f_{ZGV2} [7, 2, 8]. The SAW phase velocity is $c_{\mathrm{SAW}} = 2\pi f_{\mathrm{SAW}}/k_{\mathrm{pat}}$. The approximation from reference [12] can be used to calculate c_{T} from c_{SAW} and ν. The longitudinal sound speed can then be calculated with $c_{\mathrm{L}} = c_{\mathrm{T}}\sqrt{(2\nu-2)/(2\nu-1)}$. Finally, h can be obtained from c_{L}, ν and f_{ZGV1} using $h = \beta(\nu)c_{\mathrm{L}}/(2f_{\mathrm{ZGV1}})$. The parameter $\beta(\nu)$ is the ratio between ZGV frequency f_{ZGV1} and fundamental longitudinal thickness resonance frequency, which only depends on ν [7, 13]. It can be obtained from numerical solutions to the Rayleigh-Lamb equations.

Setup

The developed setup is depicted in Figure 2. A pulsed excitation laser (Bright Solutions Wedge HB 1064) with pulse energies of $E_{\mathrm{p}} \approx 2\,\mathrm{mJ}$ is directed through a diffractive 1:50 beam splitter (HOLO/OR MS-814-I-Y-A) followed by a cylindrical lens ($f = 130\,\mathrm{mm}$) and a dichroic mirror to produce a pattern of 50 lines on the sample's surface, which is placed in the focal plane of the lens. As depicted in Figure 2, the overall size of the generated pattern is $d = 3.7\,\mathrm{mm}$, while the line spacing is $\lambda_{\mathrm{pat}} = 76\,\mu\mathrm{m}$. This results in an excited SAW with wavenumber of $k_{\mathrm{SAW}} = 82.7/\mathrm{mm}$ (purple cross in Figure 1) and simultaneous coupling into ZGVs for samples with ZGV wavelengths $2\pi/k_{\mathrm{ZGV}} \gg d$. This is the case for $\approx 2\,\mathrm{mm}$ thick aluminum plates as displayed in Figure 1.

To detect the out-of-plane displacements, due to the vibrations induced by the excitation laser, the detection beam of a two-wave mixing interferometer (Sound & Bright Tempo) is focused on the sample through the dichroic mirror with the excitation beam. The detection beam is located in the center of the pattern. For each measurement we averaged 1000 signals, which took 1 s per point at the set pulse repetition rate of 1 kHz.

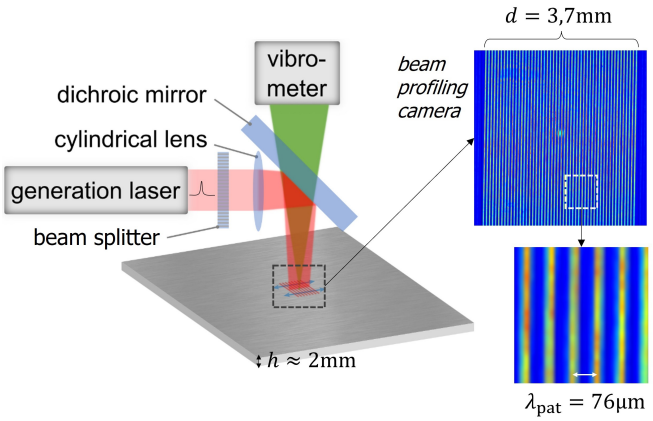

Figure 2: Experimental laser-ultrasound setup with a periodic excitation pattern for simultaneous generation and detection of ZGV resonances and one SAW with wavenumber $k_{\mathrm{SAW}} = 2\pi/\lambda_{\mathrm{pat}}$.

Signal processing

A typical signal recorded by this setup is displayed in the first row of Figure 3.

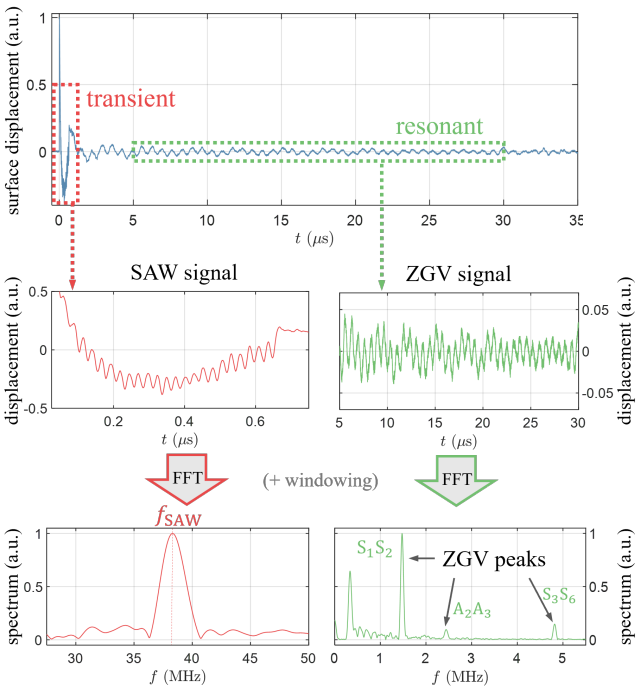

Figure 3: Signal processing for obtaining ZGV resonance frequencies f_{S1S2}, f_{S3S6}, and a SAW frequency f_{SAW} from a laser-ultrasonic measurement as displayed in Figure 2.

Since the generated SAW propagates away from the excitation region with the SAW speed c_{SAW}, its contribution to the signal is restricted to the first 0.7 µs of the sig-

nal. Therefore, as shown in the left column of Figure 3, its frequency f_{SAW} can be determined by calculating the spectrum of only this early signal portion, and determining the peak position by fitting or simple maximum search.

The signal of the locally resonant ZGV modes is still present after transient modes have propagated away from the source. Their resonance frequency can be determined by analyzing the later signal components, as shown in the right column of Figure 3. Although the A_2A_3 resonance is also included in the measured spectrum, we consider only the S_1S_2 and S_3S_6 peak for further evaluation, since two resonances are sufficient and these have the highest amplitude. For materials with other Poisson's ratios, a different choice of ZGV resonances may be more suitable.

The line spacing λ_{pat} was determined previously with a beam profiling camera placed at the same focal distance as the sample (Figure 2). With this additional information c_{L}, c_{T} and h can be calculated from the measured frequencies with the procedure outlined above.

Experiments and results

Demonstration 1: Thickness steps

For a first demonstration two thickness steps of about $\Delta h \approx 15\,\mu\mathrm{m}$ were milled into an aluminum alloy sheet (AA7075-T6). The sample was scanned relative to the excitation pattern and detection spot so that measurements were made at all three step heights. A surface displacement signal was recorded at each scan position and from its spectrum f_{S1S2}, f_{S3S6} and f_{SAW} was determined to calculate c_{L}, c_{T} and h.

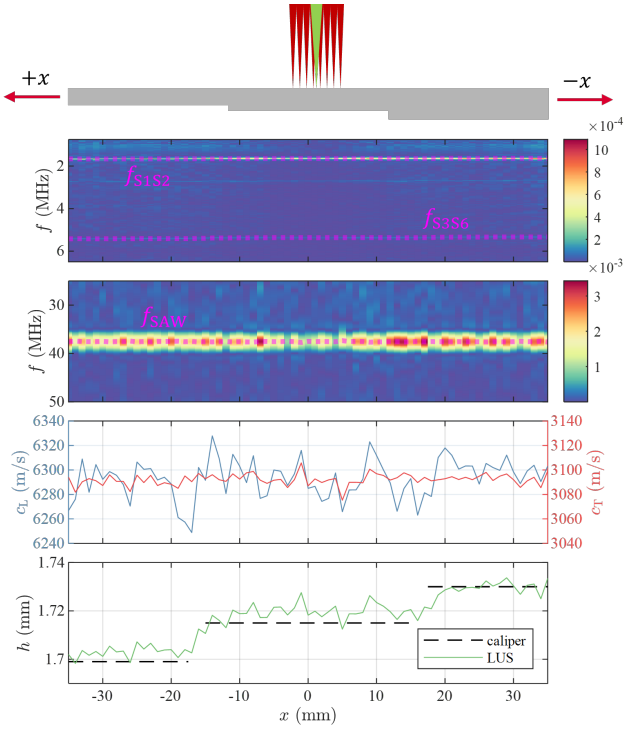

Figure 4: Results for c_{L}, c_{T} and h measured with LUS at different positions of an AA7075 aluminum plate with two thickness steps of about $\Delta h \approx 15\,\mathrm{mm}$ milled into it.

The results in Figure 4 show, that the height steps could be resolved with LUS and match well with an ex-situ caliper measurement. Additionally, the speed of sound measurements were not noticeably affected by the height differences, which would be the case for methods relying on the measurement of resonance frequencies or propagation times only.

Demonstration 2: Variation of sound speeds by heating

For a second demonstration experiment we heated a AA7075-T6 sample (with constant thickness) with a heat gun on the side facing away from the vibrometer for 300 s and let it cool down for another 600 s. Consecutive LUS measurements were done at time intervals of 2.5 s at a fixed position without moving the sample. The temperature was logged with a thermocouple welded onto the sample near the LUS measurement position.

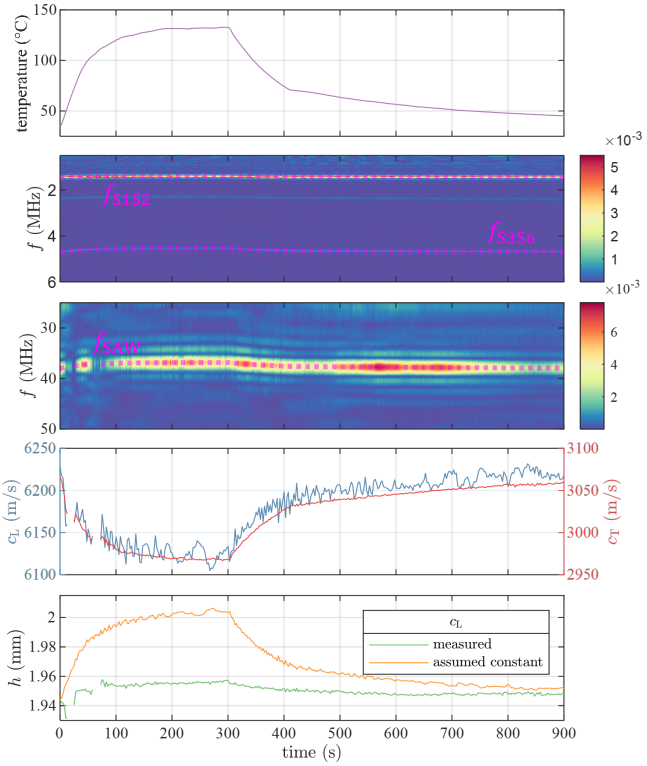

Figure 5: Results for c_{L}, c_{T} and h measured with LUS on an AA7075-T6 aluminum plate at different temperatures.

Figure 5 summarizes the results. We induced a temperature change of about $\Delta T \approx 100\,^{\circ}\mathrm{C}$, which causes changes of about 100 m/s in c_{L} and c_{T}. The thickness (green line in the bottom row of Figure 5) changes by about 5 µm, which matches well with the expected thickness increase due to thermal expansion $\Delta h = \alpha h \Delta T = 4.8\,\mu\mathrm{m}$, where $\alpha = 24\,\mu\mathrm{m}/(\mathrm{m}\,^{\circ}\mathrm{C})$ is the thermal expansion coefficient of AA7075 [14].

The evaluation shown as an orange line in Figure 5 serves as an illustration of the error made when constant sound speeds ($c_{\mathrm{L0}} = c_{\mathrm{L}}(0\,\mathrm{s})$) are assumed and only the information from the measured resonance frequencies f_{S1S2}, f_{S3S6} is used. This leads to a deviation of more than 50 µm

between the values at lowest and highest temperature, which is about 10 times larger than the value calculated from thermal expansion.

Conclusion and outlook

A laser-based method for simultaneous measurement of longitudinal and transverse sound speeds, as well as thickness of a plate is presented, which was demonstrated on an aluminum alloy sample with varying thickness. An additional demonstration shows how this enables correct thickness determination on a sample with unknown elastic properties, e.g. due to elevated temperatures.

Assuming linear increase of signal amplitude with energy, using a 100 mJ laser instead of a 2 mJ laser would lead to a SNR increase by a factor of 50. This would allow us to decrease averaging by a factor of 50^2, enabling single shot measurements while conserving SNR.

Besides technical optimizations, we aim to investigate the limitations and interplay of the pattern periodicity and grain size in metallic samples in future work. For such an investigation, we exchange the static phase mask for a dynamic spatial light modulator. This allows us to apply arbitrary patterns.

Acknowledgment

This research was funded in whole, or in part, by the Austrian Science Fund (FWF) P 33764. We thank Johannes Österreicher and Jürgen Nietsch at the AIT LKR for providing the investigated samples and invaluable materials science expertise.

References

[1] C. B. Scruby and L. E. Drain. *Laser Ultrasonics Techniques and Applications*. Taylor & Francis, 1990.

[2] Georg Watzl, Christian Kerschbaummayr, Martin Schagerl, Thomas Mitter, Bernhard Sonderegger, and Clemens Grünsteidl. In situ laser-ultrasonic monitoring of poisson's ratio and bulk sound velocities of steel plates during thermal processes. *Acta Materialia*, 235:118097, 8 2022.

[3] Karl F. Graff. *Wave Motion in Elastic Solids*. Dover Publications, 1991.

[4] Claire Prada, Dominique Clorennec, and Daniel Royer. Local vibration of an elastic plate and zero-group velocity lamb modes. *The Journal of the Acoustical Society of America*, 124:203–212, 2008.

[5] O. Balogun, T. W. Murray, and Claire Prada. Simulation and measurement of the optical excitation of the s1 zero group velocity lamb wave resonance in plates. *Journal of Applied Physics*, 102, 2007.

[6] Clemens M. Grünsteidl, István Veres, and Todd W. Murray. Experimental and numerical study of the excitability of zero group velocity lamb waves by laser-ultrasound. *The Journal of the Acoustical Society of America*, 138:242–250, 7 2015.

[7] Dominique Clorennec, Claire Prada, and Daniel Royer. Local and noncontact measurements of bulk acoustic wave velocities in thin isotropic plates and shells using zero group velocity lamb modes. *Journal of Applied Physics*, 101:1–6, 2007.

[8] Georg Watzl, Clemens Grünsteidl, Aurel Arnoldt, Jürgen A. Nietsch, and Johannes A. Österreicher. In situ laser-ultrasonic monitoring of elastic parameters during natural aging in an al-zn-mg-cu alloy (aa7075) sheet. *Materialia*, 26:101600, 2022.

[9] John A. Rogers, Martin Fuchs, Matthew J. Banet, John B. Hanselman, Randy Logan, and Keith A. Nelson. Optical system for rapid materials characterization with the transient grating technique: Application to nondestructive evaluation of thin films used in microelectronics. *Applied Physics Letters*, 71(2):225–227, 1997.

[10] Steve D. Sharples, Matthew Clark, and Mike G. Somekh. Spatially resolved acoustic spectroscopy for fast noncontact imaging of material microstructure. *Opt. Express*, 14(22):10435–10440, Oct 2006.

[11] Daniel Royer and Dominique Clorennec. An improved approximation for the rayleigh wave equation. *Ultrasonics*, 46(1):23–24, 2007.

[12] Daniel Royer and Dominique Clorennec. Theoretical and experimental investigation of rayleigh waves on spherical and cylindrical surfaces. In *1st International Symposium on Laser Ultrasonics: Science, Technology and Applications*, pages 16–18, 2008.

[13] Alexander Gibson and John S. Popovics. Lamb wave basis for impact-echo method analysis. *Journal of Engineering Mechanics*, 131(4):438–443, 2005.

[14] K.V. Shivananda Murthy, D.P. Girish, R. Keshavamurthy, Temel Varol, and Praveennath G. Koppad. Mechanical and thermal properties of aa7075/tio2/fly ash hybrid composites obtained by hot forging. *Progress in Natural Science: Materials International*, 27(4):474–481, 2017.